Video Article

# A New Technique for Quantitative Analysis of Hair Loss in Mice Using Grayscale Analysis

Tulasi Ponnapakkam[1], Ranjitha Katikaneni[1], Rohan Gulati[1], Robert Gensure[1]

[1]Pediatric Endocrinology, Children's Hospital at Montefiore

Correspondence to: Robert Gensure at rgensure@montefiore.org

URL: https://www.jove.com/video/52185
DOI: doi:10.3791/52185

Keywords: Structural Biology, Issue 97, Alopecia, Mice, Grayscale, Hair, Chemotherapy-Induced Alopecia, Alopecia Areata

Date Published: 3/9/2015

Citation: Ponnapakkam, T., Katikaneni, R., Gulati, R., Gensure, R. A New Technique for Quantitative Analysis of Hair Loss in Mice Using Grayscale Analysis. *J. Vis. Exp.* (97), e52185, doi:10.3791/52185 (2015).

## Abstract

Alopecia is a common form of hair loss which can occur in many different conditions, including male-pattern hair loss, polycystic ovarian syndrome, and alopecia areata. Alopecia can also occur as a side effect of chemotherapy in cancer patients. In this study, our goal was to develop a consistent and reliable method to quantify hair loss in mice, which will allow investigators to accurately assess and compare new therapeutic approaches for these various forms of alopecia. The method utilizes a standard gel imager to obtain and process images of mice, measuring the light absorption, which occurs in rough proportion to the amount of black (or gray) hair on the mouse. Data that has been quantified in this fashion can then be analyzed using standard statistical techniques (*i.e.,* ANOVA, T-test). This methodology was tested in mouse models of chemotherapy-induced alopecia, alopecia areata and alopecia from waxing. In this report, the detailed protocol is presented for performing these measurements, including validation data from C57BL/6 and C3H/HeJ strains of mice. This new technique offers a number of advantages, including relative simplicity of application, reliance on equipment which is readily available in most research laboratories, and applying an objective, quantitative assessment which is more robust than subjective evaluations. Improvements in quantification of hair growth in mice will improve study of alopecia models and facilitate evaluation of promising new therapies in preclinical studies.

## Video Link

The video component of this article can be found at https://www.jove.com/video/52185/

## Introduction

Alopecia (hair loss) can be a psychologically and emotionally distressing event with multiple causes. Male-pattern baldness is the most common cause of alopecia, affecting approximately two thirds of males by age 35[1]. A similar pattern of hair loss can be observed in females with polycystic ovarian syndrome. In both of these disorders, the hair loss is androgen mediated. Alopecia can also occur as an autoimmune disease, alopecia areata, which affects 1.7% of the population[2]. Alopecia can occur as a side-effect of some medical treatments, such as chemotherapy[3]. A high percentage (65-85%) of chemotherapy patients experience some degree of alopecia[4,5]. The psychological consequences of hair loss have been well studied in the chemotherapy setting. Chemotherapy-induced alopecia can result in anxiety, depression, a negative body image, lowered self-esteem and a reduced sense of well-being[6,7]. A high percentage (47-58%) of female cancer patients consider hair loss to be the most traumatic aspect of chemotherapy, and up to 8% decline treatment for fear of hair loss[4,6]. There is also evidence in androgenic alopecia to support therapy to reduce psychological and even medical consequences of hair loss[8,9]. Likewise, alopecia areata has been reported to have severe psychological consequences[2], and the patchy nature of the hair loss can lead to a more unpleasant cosmetic result than most other causes of hair loss.

While drugs with mild anti-androgenic effects (*i.e.,* spironolactone) had been used with limited success as therapy for alopecia, the first effective medication for alopecia was minoxidil[10]. This antihypertensive has an observed side-effect of causing hair growth, and is now used as topical therapy for many forms of alopecia. However, responses are often incomplete, with some subjects showing only slowing of hair loss rather than actual regrowth[10]. Finasteride is a competitive antagonist to type II 5α-reductase which blocks conversion of testosterone to dihydrotestosterone, resulting in improvements in androgenic alopecia at the expense of partial systemic androgen blockade. Response rates with long-term (10 years) therapy are around 50%[11]. Overall, despite considerable research in this area, there is still no adequate therapy for hair loss.

For decades, scientists and clinicians have examined methods of measuring scalp hair growth in clinical trials. With the development of drugs that treat alopecia, there has been a greater need for reliable, economical and minimally invasive means of measuring hair growth and, specifically, response to therapy. Image analysis technology for a precise quantification of hair density in patients with hair loss disorders yielded consistent and valid results in the past using a variety of techniques, including analysis of digitized images[12], image analysis of individual hairs and skin lesions[13], and microscopic scanning to quantify hair mass in a defined scalp region[14] .

Unfortunately, while the above methodologies have provided improved assessment of efficacy for hair growth-promoting interventions in clinical trials, these methods have not been applied to rodent studies in preclinical investigations. Our goal is to develop a consistent and reliable method to quantify hair loss in mice, which will allow investigators to more accurately assess and compare new therapeutic approaches for various

 

forms of alopecia. We have developed a methodology using equipment readily available in most laboratories which will allow rapid and reliable quantification of hair density in mice with brown or black hair. This methodology has been tested in mouse models of chemotherapy-induced alopecia, alopecia areata, and alopecia from waxing. A detailed protocol is presented for performing these measurements, including validation data from C57BL/6 and C3H/HeJ strains of mice. As this technique relies on detecting light absorption from pigments in the hair shaft, it cannot be used to detect hair growth in white mice or albino mice.

## Protocol

Ethics Statement: All studies involving animals must be approved by the IACUC of the institution (for the data which follows, protocols were approved by the Montefiore IACUC, protocol #11-6-240 and #13-7-100). Animals are provided light anesthesia as indicated for the sole purpose of keeping them still during photography, there are no painful procedures required for this protocol.

## 1. Acquisition of Photographs

1. Set focus and field of view for gel imager using paper with printed text. Verify uniformity of light source across photographed region. To help ensure uniformity, use a gel imager with a built in light source for reflective photography. Do not use a transillumination light source, as this would create a silhouette of the animal which is unsuitable for further grayscale analysis.
   NOTE: This will place the mouse slightly out of focus, which provides optical averaging across the region of interest (ROI) and will help reduce quantal errors for very small (*i.e.,* <10 pixel) regions of interest. Larger regions of interest will not be affected by this minor focusing adjustment, nor will they be affected by differences in the size of the animal.
2. Anesthetize animals using ketamine (100 mg/ml)/xylazine (20 mg/ml) (2:1), as this provides rapid anesthesia effect and rapid recovery and is optimal for photographing multiple animals.
   NOTE: Anesthesia is confirmed when the animal is still enough to permit photography. As animals typically recover from this light anesthesia within 10-15 min, the veterinarian has not recommended use of eye ointments.
3. Place anesthetized animals on gel imager in vertical alignment (as close to parallel as possible).
   1. For dorsal photographs, place the animals in prone position with limbs extended.
   2. For ventral photographs, place animals in the supine position, taking care that the animals are not laterally rotated.
4. Place grayscale standard in photographed region.
5. Close access door. Important: Ambient light can introduce variations in exposure.
6. Set F-stop to an exposure which places the region of interest within the linear range of acquisition (reading F-stop).
   NOTE: Most systems will display where the image is saturated.
7. Take photograph.
8. Change F-stop to another exposure setting which places the region of interest within the linear range by increasing or decreasing the F-stop by 1, such that both the standard and the region of interest remain in a linear range of acquisition (reference F-stop).
9. Take photograph.
10. Once photography is completed, place animals on a warming table and monitor until they can maintain sternal recumbency. Return animals to their cages. Return the group of animals to the vivarium once all animals are fully recovered.

## 2. Quantification of Light Absorption

1. Mark regions of interest on the images of the animals using provided software for gel imager.
   1. For whole animal dorsal view, use a rectangular or oval image extending from the upper limbs to the lower limbs, extending laterally as much as possible such that no part of the box extends beyond the back of the animal as shown in **Figure 1A**.
      NOTE: One could also mark the area of interest using a free-hand drawing tool.
   2. For whole animal ventral view, use 2 rectangles: one covering the pelvic region and one covering the chest area as shown in **Figure 1B**.
   3. For a smaller region of interest, *i.e.,* location of drug administration, mark as appropriate.
2. Mark region(s) of interest on grayscale absorption standard.
3. Record absorption from each of the marked regions of interest.

## 3. Analysis

Absorption levels obtained for the regions of interest may need to be normalized to the background standard for comparison between photographs. The relationship of exposure to absorption is log-log (*i.e.,* the relationship is linear between log(exposure) and log(absorption)). Using this relationship, the absorption of the region of interest can be normalized to a standard background value, which will allow absorptions to be compared directly between different photographs, including those taken at different time points (*i.e.,* serial measurements within a study protocol). The procedure for performing these corrections is detailed in optional steps 3.1 and 3.2.

1. (Optional) Plot curve of log (exposure) *vs.* log(absorption) using values obtained from grayscale absorption standard.
2. (Optional) Adjust for variations in the standard of each photograph as follows:
   1. Select F-stop for reading (as determined in step 1.6) and F-stop for reference (as determined in step 1.8).
   2. Calculate average absorption of the standard in all photographs at the reading F-stop. This average is the Reference Standard Value (RSV).
   3. Calculate difference in absorption between the reading and reference F-stop settings in each photograph for the standard (delta-S) and for each defined ROI (delta-ROI-1, delta-ROI-2 …..delta-ROI-X)

 

4. Calculate the corrected absorption for each ROI as follows: Corrected absorption (ROI-X) = Absorption (ROI-X) at reading F-stop + (RSV - absorption of standard at reading F-stop) * (delta-ROI-X /delta-S)

3. Compile experimental data and perform data analysis using standard statistical techniques for continuous variables (*i.e.,* ANOVA, T-test).

## Representative Results

This technique was validated using C3H/HeJ engrafted mice, the mouse model of alopecia areata[16]. These animals develop global hair loss which progresses gradually over time. However, the hair loss occurs in patches, and may vary from one mouse to the next, introducing considerable variability and hampering qualitative assessments. This model provided an opportunity to test correlations between measurements of optical density at different locations on the mouse as an assessment of validity.

The first question was if measures using different exposures, variations in ROI demarcation, and ROI's from non-overlapping areas on the same mouse were correlated. There was a significant correlation ($p < 0.0001$) seen comparing ROIs defined by rectangular *vs.* oval standards on the dorsal surface of the mouse (**Figure 4A**). Similarly high correlations were seen at different sites on the animal and at different exposure levels (not shown). This indicates a high degree of precision in these measurements. There was also a significant correlation between absorption at F-stop 2.0 *vs.* 1.2 on the dorsal surface of the back using rectangular ROIs ($p < 0.0001$, **Figure 4B**). A significant correlation was observed even when comparing absorption measurements between the dorsal and ventral surface of the same mouse ($p < 0.0001$, **Figure 4C**). These data provide evidence that absorption measurements taken from different sites on the same animal are correlated, as expected in the C3H/HeJ engrafted mouse model, and these correlations remain linear across a wide range of hair loss. This helps establish validity of the grayscale measurements and also establishes robustness of this technique to variations in image acquisition and analysis technique.

The second question was if there is consistency between serial measurements taken from the same animal at different time points. To assess this, images were obtained of C3H/HeJ engrafted mice on a weekly basis for 3 weeks. The C3H/HeJ engrafted mouse would be expected to display gradual hair loss over this time. Grayscale analysis on the ventral surface (chest region, box-shaped ROI) showed this expected hair loss, with consistent downward trend from one time point to the next (**Figure 5**). Of note, only 80% of C3H/HeJ engrafted mice show hair loss, and those with the highest grayscale values do not show this decline, rather exhibit consistent results across the experimental period. This consistency of measure in animals with no hair loss was also verified in the C57BL/6 mouse[19]. The same analysis performed on the thigh region of the ventral surface and on the dorsal surface showed similar results across time (not shown).

With these encouraging results from application of this technique in C3H/HeJ engrafted animals, further investigations were conducted in a different animal model, one of chemotherapy-induced alopecia. C57BL/6 mice which receive 3 weekly courses of cyclophosphamide will variably develop global hair thinning and depigmentation. The grayscale analysis technique described herein was employed to quantify these changes, and to assess response to therapeutic interventions[17]. In this model, the grayscale analysis proved to be a powerful tool in providing quantitative assessments of chemotherapy-induced changes in hair coat, and permitted verification of treatment effects by statistical analysis. In another model of chemotherapy alopecia, there were special challenges in utilizing this grayscale analysis. In this model, animals are waxed on the dorsal surface to synchronize the hair follicles, then treated with a single dose of cyclophosphamide 9 days later, when hair follicles have entered anagen VI stage and are maximally sensitive to chemotherapeutics[18]. The waxed region is the region of interest for study, but the area of waxing might be of variable size. Restricting the ROI to within the waxed region permits quantification of both loss and regrowth of hair after cyclophosphamide administration[19]. Furthermore, the technique permits accurate assessment of dose-dependent differences in treatment response of an experimental therapy. This application illustrates the advantages of having flexibility in defining the ROI in this technique.

To further illustrate the application of this technique, provided are an interim data analysis of an ongoing study in C57BL/6 utilizing the protocol of weekly cyclophosphamide administration indicated above. 8 week old mice were treated with vehicle or 50 mg/kg/wk cyclophosphamide for 3 weeks. Chemotherapy-treated mice showed visually apparent hair loss after 2 months, while vehicle-treated animals had a normal hair coat (**Figure 6A**). Grayscale analysis was performed as indicated above, showing significant ($p < 0.05$) difference between chemotherapy mice and vehicle controls (**Figure 6B**).

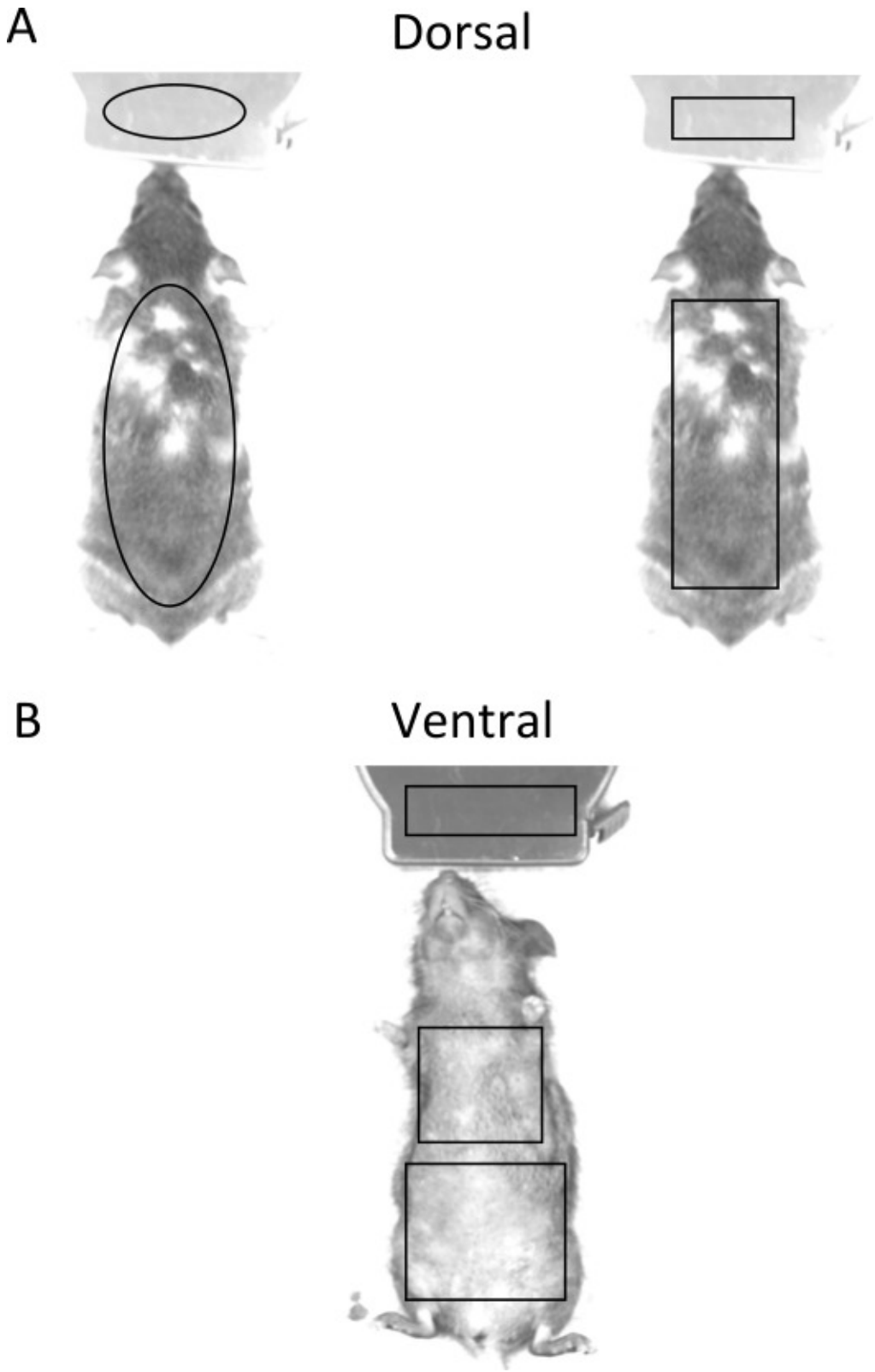


**Figure 1: Gross view of hair changes on the dorsal and ventral surface of C3H/HeJ engrafted mice, the mouse model of alopecia areata.** Note the animals develop global hair loss which progresses gradually over time. **(A)** Dorsal view, with representative demarcation of regions of interest (ROIs) for grayscale analysis, oval or rectangular as indicated. **(B)** Ventral view with different regions of interest for grayscale analysis in chest, corresponding to an ungroomed area, or thigh, corresponding to a groomed area.

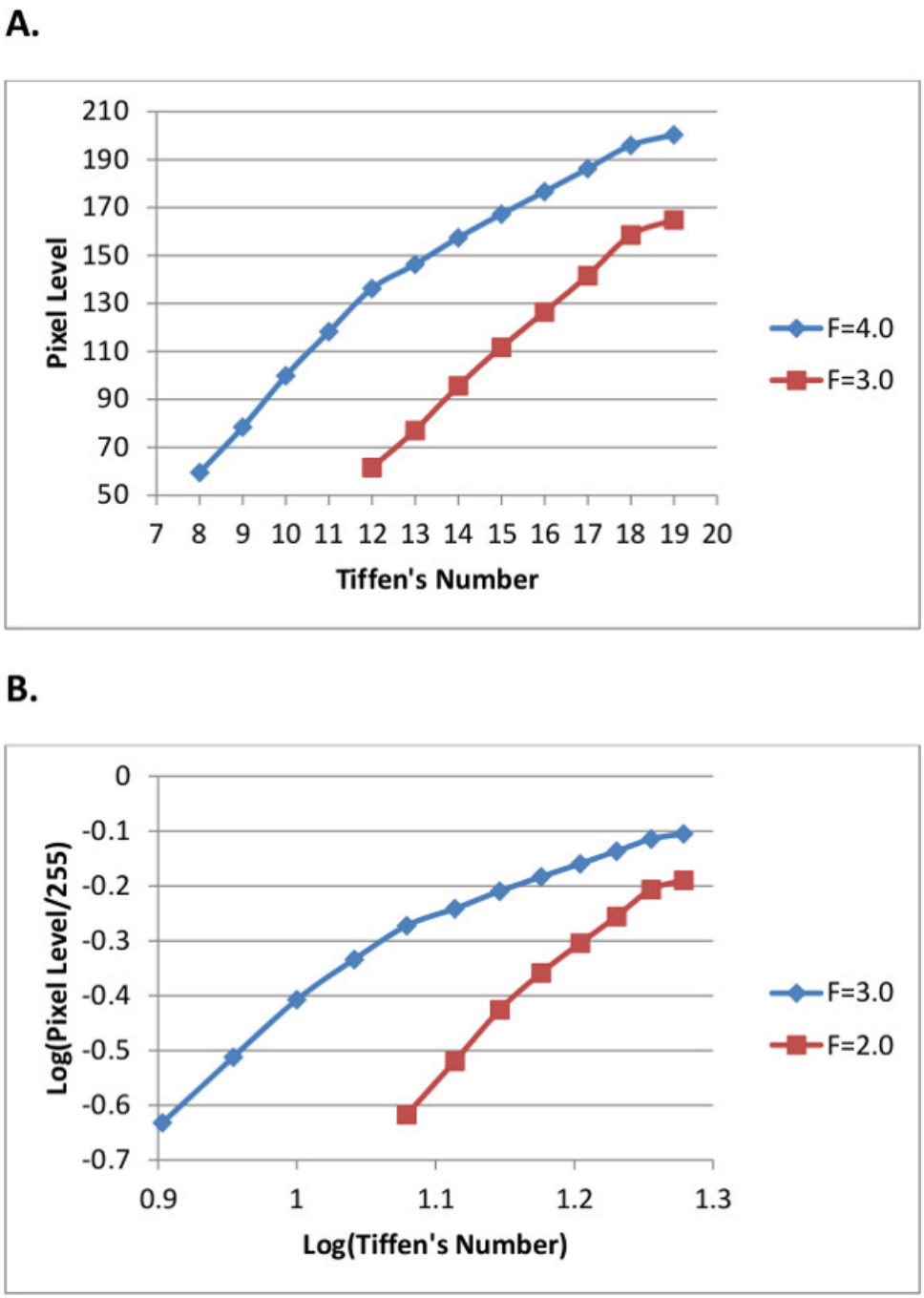


**Figure 2: Pixel level on grayscale analysis *vs.* Tiffen's number standard.** A standard Tiffen's chart was photographed on a gel imager at the indicated F-stops. **(A)** Graph of Pixel level *vs.* Tiffen's number, showing expected logarithmic relationship. **(B)** Logarithmic transformation, in this range continues to follow a nonlinear relationship.

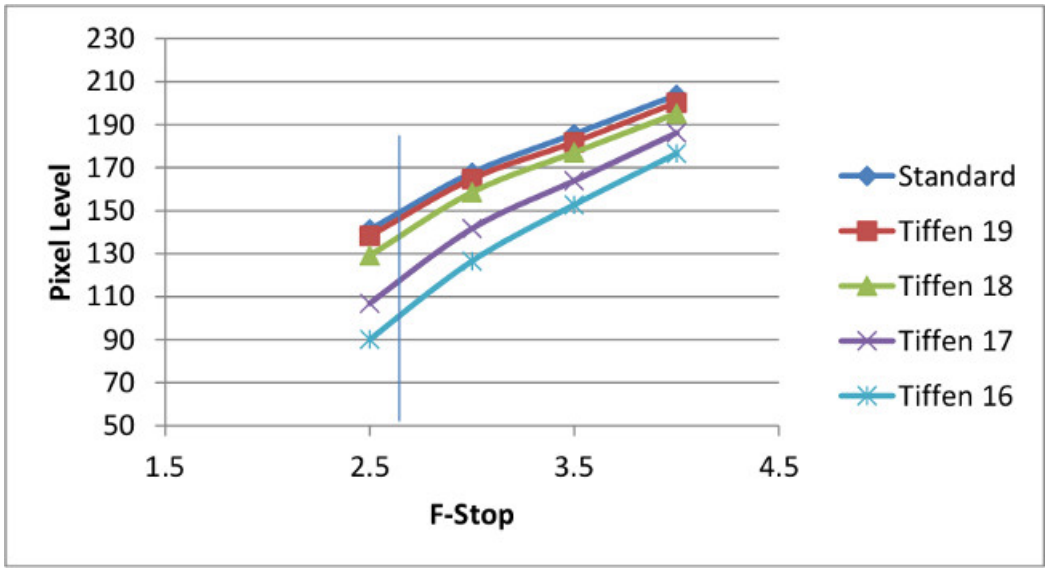


**Figure 3: Pixel level on grayscale analysis *vs.* F-stop.** A standard Tiffen's chart was photographed on a gel imager at the indicated F-stops. Plotted are the variations in pixel level seen for several different Tiffen's standards *vs.* F-stop. Note that the lines are not parallel, indicating that corrections to align standards between photographs need to be individually calculated for each region of interest.

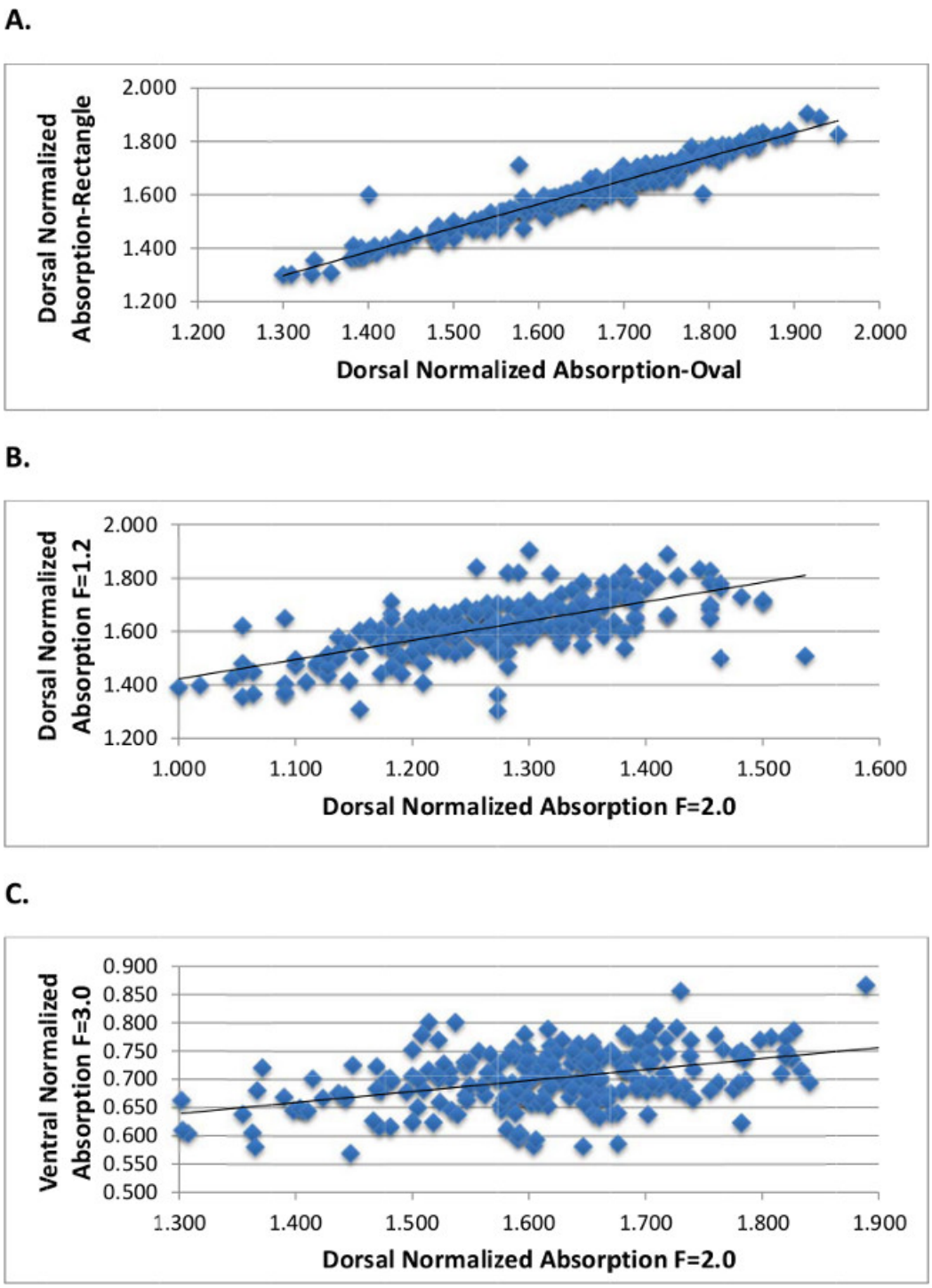


**Figure 4: Correlation between different photographic techniques and regions of interest in grayscale analysis.** Shown are correlations between the indicated measurement techniques taken from the same C3H/HeJ engrafted mouse at the same time point. **(A)** Correlation of rectangle vs. oval region of interest on the dorsal view. **(B)** Correlation of F stop 2.0 *vs.* 1.2 using rectangular region of interest. **(C)** Correlation of grayscale values from dorsal and ventral views, rectangular region of interest. All correlations were statistically significant as determined by linear regression analysis ($p < 0.0001$).

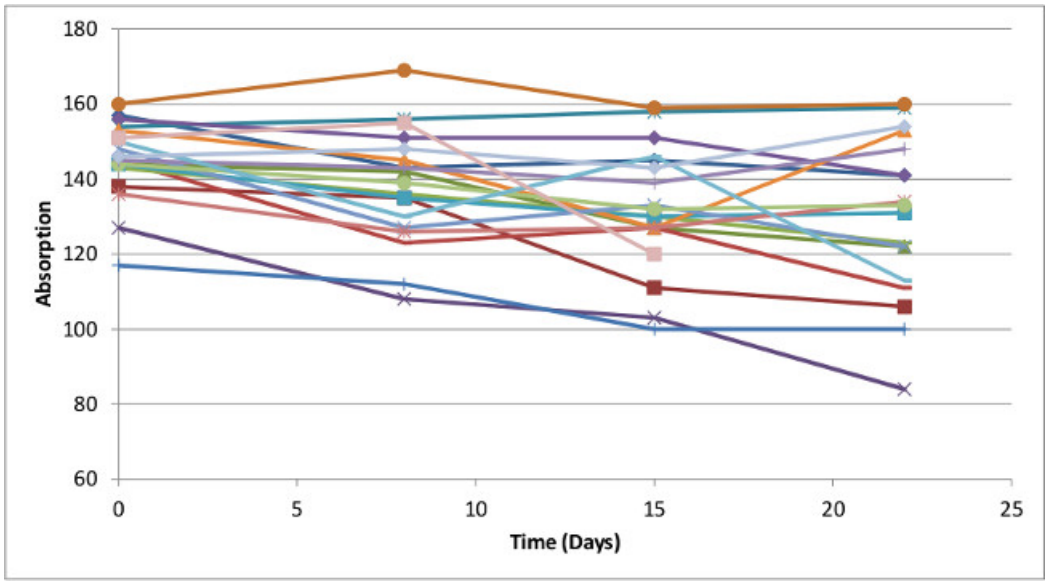


**Figure 5: Time course of change in absorption using grayscale analysis in C3H/HeJ engrafted mice.** Colors indicate serial measurements from individual mice. Note the consistency for each mouse from one time point to the next.

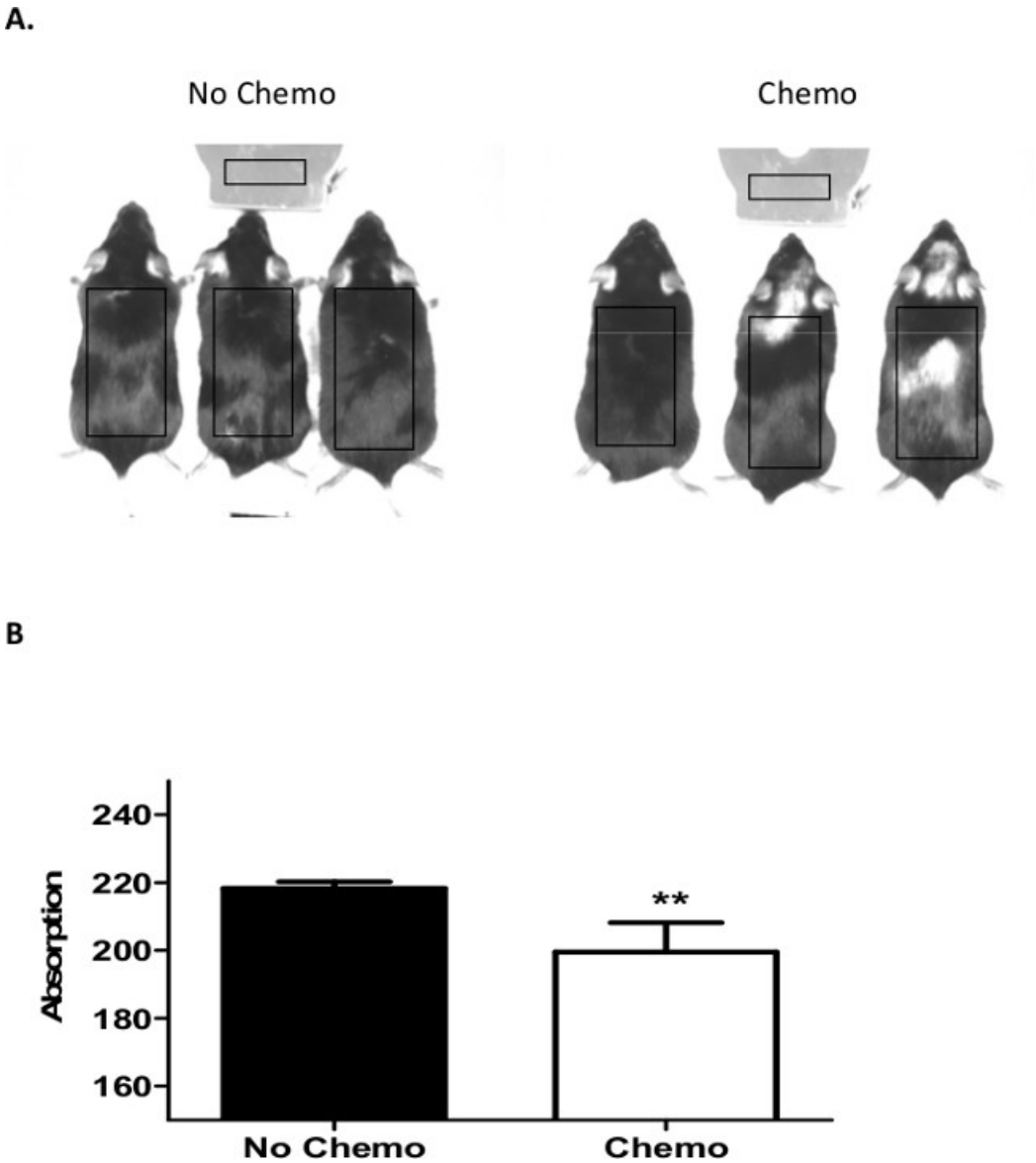


**Figure 6: Grayscale analysis in chemotherapy-induced alopecia.** 6-week old C57BL6/J mice were treated with either vehicle (N = 6) or 3 weekly doses of cyclophosphamide (50 mg/kg) (N=6). **(A)** Representative group of 3 mice from each of the treatment groups, photographed 2 months after the start of chemotherapy. **(B)** Compiled data from grayscale analysis from each group, showing decreased absorption with cyclophosphamide administration ($p < 0.05$). Note the correlation between visible hair loss in panel A and statistically significant reductions in absorption in panel B.

| Absorption values are as follows: | | | |
|---|---|---|---|
| Photograph | F-stop | ROI | Absorption |
| 1 | 2 | Standard | 90 |
| 1 | 2 | ROI-1 | 100 |
| 1 | 2 | ROI-2 | 200 |
| 1 | 3 | Standard | 150 |
| 1 | 3 | ROI-1 | 160 |
| 1 | 3 | ROI-2 | 230 |
| 2 | 2 | Standard | 110 |
| 2 | 2 | ROI-1 | 120 |
| 2 | 2 | ROI-2 | 210 |
| 2 | 3 | Standard | 160 |
| 2 | 3 | ROI-1 | 170 |
| 2 | 3 | ROI-2 | 235 |
| Reading F-stop chosen as 2.0, Reference F-stop chosen as 3.0. | | | |
| Reference Standard Value (RSV) = average of absorption of standard from photograph 1 and photograph 2 at F-stop 2.0, RSV=average(90, 110) = 100 | | | |
| | | | |
| For photograph 1: | | | |
| Delta-S = 150 - 90 = 60 | | | |
| Delta-ROI-1 = 160 - 100 = 60 | | | |
| Delta-ROI-2 = 230 - 200 = 30 | | | |
| Corrected absorption for ROI-1 = 100 + (100 - 90) * (60 / 60) = 110 | | | |
| Corrected absorption for ROI-2 = 200 + (100 - 90) * (30 / 60) = 205 | | | |
| | | | |
| For photograph 2: | | | |
| Delta-S = 160 - 110 = 50 | | | |
| Delta-ROI-1 = 170 - 120 = 50 | | | |
| Delta-ROI-2 = 235 - 210 = 25 | | | |
| Corrected absorption for ROI-1 = 120 + (100 - 110) * (50 / 50) = 110 | | | |
| Corrected absorption for ROI-2 = 210 + (100 - 110) * (25 / 50) = 205 | | | |

**Table 1: Sample calculation for correcting differences in exposure between photographs.** The table shows an example of how to compensate for minor differences in absorption of the standards between photographs (optional step 3.2).

## Discussion

In this report a detailed description is provided of a new technique for quantifying hair loss in rodents. This technique utilizes a gel imager for image acquisition and analysis, equipment which is readily available in most laboratories. The measurements have been shown to be robust to minor variations in technique (**Figures 4**-**5**), and are well-correlated to the degree of visual hair loss in treatment models (**Figure 6**). These techniques have been successfully employed in evaluation of experimental therapies for alopecia[17].

A quantitative tool for assessing hair growth in rodents can be very valuable in advancing research in therapeutics for alopecia. Many mouse models for alopecia have intrinsic variability, which makes it difficult to base results on subjective assessments of therapeutic interventions. Likewise, a quantitative assessment which provides a result in the form of a continuous measure can be summarized by group averages and standard deviation/standard error, and can be tested using standard statistical techniques (ANOVA, T-test). This quantitative assessment can be utilized to measure responses over a series of time points, and can be used in generating a dose-response curve for a test compound. Quantitative analysis thus allows for evidence-based assessments of efficacy of therapeutics which are under development.

This technique takes advantage of the difference in color between hair coat and skin present in many mouse strains. For mice with dark hair, the greater the density of the hair, the greater amount of optical absorption. This optical absorption can be quantified using a gel imaging apparatus, which is designed to assess optical absorption in a defined region of interest to quantify protein amounts in western blot analysis. Similar to western blot analysis, the resulting absorption measurements can be analyzed using standard statistical methods to compare hair density between groups of mice (*i.e.,* treatment vs. control).

Western blot analysis is generally performed on a single image which is analyzed compared to standards provided on that image. However, with this application, it becomes necessary to make comparisons between different images, which may be taken at different times. With very consistent photographic technique, variations between photographs can be minimized. However, for experimental application, it is helpful if minor variations in exposure between photographs can be compensated for. Thus, it is important that a grayscale standard be included in the photograph (*i.e.,* Tiffen's grayscale chart[15]). However, the relationship between absorption and exposure varies depending on the optical density of the target (**Figure 2A**). Thus, if the grayscale standard has a different optical density from the target, the appropriate corrections may be different. Logarithmic corrections are helpful, but do not provide a perfect solution to this problem (**Figure 2B**). By taking photographs at 2 different F-stops, one can calculate a linear approximation for the grayscale standard and for each target on the photograph, and thus provide an appropriate scaling of the correction for the individual targets. **Figure 3** illustrates how targets with different optical densities will have different correction factors, which can be interpolated from differences in absorption of each target at 2 different F-stops. Thus, if one wishes to normalize the standard to value of 150, a target at optical density Tiffen 19 would be 148, one at Tiffen 18 would be 140, one at Tiffen 17 would be 119, and so on. Rather than resolving these corrections graphically, one can use a ratio of slopes between the grayscale standard and the target between the 2 F-stops to calculate the correction for each target, as explained in the provided example (**Table 1**).

Like all techniques, quantitative analysis of hair growth through grayscale analysis has several limitations. First and foremost, there is significant computational complexity in application of this technique. This results from the fact that the analysis software for gel imagers is optimized for analyzing each figure as a separate experiment. Thus, there is a requirement to manually correct for any variation in exposures between images. The linearized approximation for such corrections does help simplify this process. An example is provided in **Table 1**: Simulated data of 2 sets of photographs, taken at F-stop 2.0 and 3.0, with a common standard. Each set of photographs has 2 ROIs which need to be compared between sets. Minor variations in photographic conditions have caused the first set of photographs to have a slightly greater exposure than the second set, evident by minor differences in the absorption of the common standard.

The example shows how minor differences in photographic conditions can create apparent differences in absorption at a given ROI, but these can be corrected using a reference standard, in this case showing that absorption at the ROIs do not differ between the 2 sets of images.

It is important to note that change in light absorption does not always directly correlate to quantity of hair depigmentation or other color changes might be mistaken for hair loss or hair growth. Unfortunately, the accuracy of this technique cannot be assessed because there is currently no gold standard with which to compare. However, where there is obvious hair loss, the technique does produce the expected results (**Figure 6**). Lastly, there is currently no data to assess if results using this technique correlate with outcomes in clinical trials of potential therapeutics.

The grayscale analysis for quantifying hair loss in various forms of alopecia represents an opportunity to refine and standardize methods for characterizing models of alopecia and for testing responses to potential therapeutics. Application of this technique should enhance identification and development of more effective therapies for alopecia.

## Disclosures

Authors have nothing to disclose.

## Acknowledgements

We would like to thank the Children's Hospital at Montefiore, Department of Pediatrics, for providing support for these studies. We would like to thank the National Alopecia Areata Foundation for providing financial support for conducting studies with C3H/HeJ engrafted mice.

## References

1. McAndrews, P. J. American Hair Loss Association. http://www.americanhairloss.org/men_hair_loss/introduction.asp (2011).
2. Safavi, K. H., Muller, S. A., Suman, V. J., Moshell, A. N., Melton, L. J. 3rd Incidence of alopecia areata in Olmsted County, Minnesota, 1975 through 1989. *Mayo Clin Proc.* **70**, (7), 628-633 (1995).
3. Hussein, A. M. Chemotherapy-induced alopecia: new developments. *South Med J.* **86**, (5), 489-496 (1993).
4. Trueb, R. M. Chemotherapy-induced hair loss. *Skin Therapy Lett.* **15**, (7), 5-7 (2010).
5. Sato, N., Leopold, P. L., Crystal, R. G. Effect of adenovirus-mediated expression of Sonic hedgehog gene on hair regrowth in mice with chemotherapy-induced alopecia. *J Natl Cancer Inst.* **93**, (24), 1858-1864 (2001).
6. McGarvey, E. L., Baum, L. D., Pinkerton, R. C., Rogers, L. M. Psychological sequelae and alopecia among women with cancer. *Cancer Pract.* **9**, (6), 283-289 (2001).
7. Baxley, K. O., Erdman, L. K., Henry, E. B., Roof, B. J. Alopecia: effect on cancer patients' body image. *Cancer Nurs.* **7**, (6), 499-503 (1984).
8. Stough, D. Psychological effect, pathophysiology, and management of androgenetic alopecia in men. *Mayo Clin Proc.* **80**, (10), 1316-1322 (2005).
9. Ogunmakin, K. O., Rashid, R. M. Alopecia: the case for medical necessity. *Skinmed.* **9**, (2), 79-84 (2011).
10. Olsen, E. A. A randomized clinical trial of 5% topical minoxidil versus 2% topical minoxidil and placebo in the treatment of androgenetic alopecia in men. *J Am Acad Dermatol.* **47**, (3), 377-385 (2002).
11. Rossi, A. 1 mg daily administration on male androgenetic alopecia in different age groups: 10-year follow-up. *Dermatol Ther.* **24**, (4), 455-461 (2011).
12. Gibbons, R. D., Fiedler-Weiss, V. C. Computer-aided quantification of scalp hair. *Dermatol Clin.* **4**, (4), 627-640 (1986).
13. Fleming, M. G. Techniques for a structural analysis of dermatoscopic imagery. *Comput Med Imaging Graph.* **22**, (5), 375-389 (1998).
14. Chamberlain, A. J., Dawber, R. P. Methods of evaluating hair growth. *Australas J Dermatol.* **44**, (1), 10-18 (2003).
15. *The Kodak/Tiffen Q-13 Gray Scale*.* Imatest http://www.imatest.com/docs/q13/ Forthcoming.
16. Freyschmidt-Paul, P. Treatment of alopecia areata in C3H/HeJ mice with the topical immunosuppressant FK506 (Tacrolimus). *Eur J Dermatol.* **11**, (5), 405-409 (2001).

 

17. Katikaneni, R., Ponnapakkam, T., Matsushita, O., Sakon, J., Gensure, R. Treatment and prevention of chemotherapy-induced alopecia with PTH-CBD, a collagen-targeted parathyroid hormone analog, in a non-depilated mouse model. *Anticancer Drugs.* **25**, (1), 30-38 (2014).
18. Peters, E. M., Foitzik, K., Paus, R., Ray, S., Holick, M. F. A new strategy for modulating chemotherapy-induced alopecia, using PTH/PTHrP receptor agonist and antagonist. *J Invest Dermatol.* **117**, (2), 173-178 (2001).
19. Katikaneni, R., Ponnapakkam, T., Seymour, A., Sakon, J., Gensure, R. C. Parathyroid hormone linked to a collagen binding domain promotes hair growth in a mouse model of chemotherapy induced alopecia in a dose-dependent manner. *Anti-cancer drugs.* **25**, (7), 819-825 (2014).

 